BIOCELL
2024 48(10): 1503-1516
ARTICLE

Tech Science Press

Diosgenin inhibited podocyte pyroptosis in diabetic kidney disease by regulating the Nrf2/NLRP3 pathway

Yu TANG[1]; Wenxiao HU[2,*]; Yajun PENG[1]; Xiangdong LING[2]

[1] Department of Nephrology, The First Hospital of Hunan University of Chinese Medicine, Changsha, 410007, China
[2] Department of Endocrinology, The First Hospital of Hunan University of Chinese Medicine, Changsha, 410007, China

Key words: Diosgenin, Nrf2, NLRP3, Diabetic kidney disease, Pyroptosis

Abstract: Background: Podocyte injury is crucial in diabetic kidney disease (DKD) progression, and the mechanism remains unclear. The previous studies indicated Diosgenin played a key role in inhibiting podocyte injury progression. However, more research is needed to explore Diosgenin in inhibiting-molecular mechanisms in the process of podocyte injury. **Methods:** The content of Diosgenin in HeShenwan was detected by High-Performance Liquid Chromatography-mass spectrometry (HPLC-MS) method. The podocyte injury model was constructed by high glucose (HG)-induced mpc5 cells. The Cell Counting Kit-8 (CCK-8) assay was utilized to evaluate the activity of mpc5 cells. Pyroptosis in mpc5 cells was assessed using flow cytometry. Molecular docking studies of Diosgenin and Nrf2 were carried out using VINA 1.1.2 software. The levels of Superoxide dismutase (SOD), Malondialdehyde (MDA), Reactive oxygen species (ROS), Interleukin 1β (IL-1β), Interleukin 18 (IL-18), Lactate dehydrogenase (LDH) and High mobility group protein B1 (HMGB1) were assessed using related kits. The levels of Nod-like receptor protein 3 (NLRP3), Nuclear factor erythroid-2-related factor 2 (Nrf2), Cysteinyl aspartate specific proteinase 1 (Caspase-1), Gasdermin (GSDMD), and Apoptosis-associated speck-like protein contain a CARD (ASC) were detected. **Results:** The Diosgenin content was the highest in HeShenwan. The addition of Diosgenin enhanced HG-induced mpc5 cell activity and reduced oxidative stress and pyroptosis. Molecular docking results showed that Diosgenin bound to the Nrf2 through hydrogen bonds and hydrophobic interactions, regulating the Nrf2 expression. Overexpression of Nrf2 reduced the levels of NLRP3, reducing oxidative stress and inhibiting pyroptosis in mpc5 cells. Knockdown of Nrf2 reduced HG-induced mpc5 cell activity and increased pyroptosis and oxidative stress. Diosgenin inhibited pyroptosis in mpc5 cells by regulating the Nrf2/NLRP3 pathway. **Conclusion:** Diosgenin inhibited HG-induced pyroptosis in mpc5 cells by regulating the Nrf2/NLRP3 pathway.

Abbreviations

DKD	Diabetic kidney disease
HPLC-MS	High-Performance Liquid Chromatography-mass spectrometry
HG	High glucose
SOD	Superoxide dismutase
ROS	Reactive oxygen species
MDA	Malondialdehyde
IL-1β	Interleukin 1β
IL-18	Interleukin 18
LDH	Lactate dehydrogenase
HMGB1	High mobility group protein B1
NLRP3	Nod-like receptor protein 3
Nrf2	Nuclear factor erythroid-2-related factor 2
Caspase-1	Cysteinyl aspartate specific proteinase 1
GSDMD	Gasdermin
ASC	Apoptosis-associated speck-like protein contain a CARD
CKD	Chronic kidney disease
SIRT6	Sirtuin 6
AMPK	AMP-activated protein kinase
HO-1	Heme oxygenase-1
FBS	Fetal bovine serum
OD	Optical density
STING	Stimulator of interferon genes
IRF3	Interferon regulatory transcription factor 3
WDR5	WD repeat-containing protein 5

*Address correspondence to: Wenxiao Hu, huwenxiao110@hnucm.edu.cn
Received: 11 April 2024; Accepted: 18 June 2024;
Published: 02 October 2024

Doi: 10.32604/biocell.2024.052692

www.techscience.com/journal/biocell

DOT1L	DOT1-like histone H3K79 methyltransferase
GBM	Glomerular basement membrane
EDTA	Ethylene diamine tetraacetic acid

Introduction

Diabetic kidney disease (DKD) is a diabetes-induced condition that damages the kidneys and is a major factor in chronic kidney disease (CKD) [1,2]. The main treatment approaches for DKD mainly relied on methods such as hemodialysis, peritoneal dialysis, and kidney replacement therapy (kidney transplant). These treatments eased kidney damage and slowed down the DKD progression [3]. Due to DKD's complex pathogenesis, the lack of specific treatments in clinical practice results in around half of type 2 diabetes and one-third of type 1 diabetes developing into CKD [4]. Therefore, exploring the pathogenesis of DKD and developing a specific treatment approach was crucial. Podocytes were vital elements of the glomerular filtration barrier in conjunction with endothelial cells and the glomerular basement membrane (GBM) [5]. Podocyte injury was crucial in DKD progression [6,7]. Nevertheless, the mechanism of podocyte injury in DKD remained unclear.

Pyroptosis is a particular kind of programmed cell death that is typified by the swelling and rupture of cells, which releases inflammatory chemicals from the cell and sets off an inflammatory response. Research has found a mechanistic association between pyroptosis and podocyte injury in DKD [8]. Pyroptosis could activate the NLRP3 inflammasome. Furthermore, research indicated that the NLRP3 inflammasome was activated in DKD, and downregulation of NLRP3 expression could alleviate diabetic kidney damage [9,10]. Activation of the inflammasome led to Caspase-1 activation, resulting in the cleavage of gasdermin-D (GSDMD) into GSDMD-N, thereby initiating pyroptosis [11]. Nrf2 is essential for the cellular regulation of oxidative stress as the primary signal for clearing intracellular ROS to combat oxidative stress. Studies indicated that Nrf2 delayed the progression of DKD by exerting anti-inflammatory and antioxidant damage effects, reducing mitochondrial damage, and making it one of the therapeutic targets for DKD [12]. In osteoarthritis, silencing Nrf2 led to the upregulation of NLRP3 expression, while knocking down NLRP3 did not affect Nrf2 expression [13]. Additionally, syringaresinol could upregulate Nrf2 to regulate NLRP3 expression and thereby inhibit pyroptosis [14]. The above studies indicated that the Nrf2/NLRP3 pathway significantly influenced pyroptosis.

HeShenwan is composed of Chinese yam, astragalus complanatus, lotus seed, oyster shell, ossa draconis, gordon euryale, Chinese date, golden cypress, and sticky rice. It has been proven to have a curative effect on primary nephropathy in the clinic. Yam is a perennial rhizome plant of Dioscorea in Dioscoreaceae. Diosgenin is an active monomer in plants of Dioscoreaceae, such as yam. Diosgenin has many biological activities, such as lipid and glucose metabolism regulation, anti-oxidation, anti-inflammatory, anti-proliferation, and anti-tumor effects [15,16]. Studies have shown that Diosgenin prevented podocyte injury in the early stage of DKD by regulating Sirtuin 6 (SIRT6) [15]. At the same time, Diosgenin protected the retinal pigment epithelial (ARPE-19) cells from inflammatory damage and oxidative stress brought on by high glucose (HG) via inducing the AMP-activated protein kinase/Nrf2/Heme oxygenase-1 (AMPK/Nrf2/HO-1) pathway [17]. Another study has shown that regulating the NLRP3 pathway could inhibit the inflammatory response of RAW264.7-derived foam cells [18]. Nevertheless, whether Diosgenin could affect podocyte pyroptosis in DKD by influencing Nrf2/NLRP3 to inhibit podocyte injury has not been reported.

Against the above background, we hypothesized Diosgenin's significant role in DKD progression and investigated its mechanism.

Materials and Methods

Cell culture

Mouse kidney podocytes mpc5 cells (Immocell Biotechnology, IM-M011, Xiamen, China) were cultured in RPMI 1640 medium (Abiowell, AW-M018, Changsha, China) containing 10% Fetal Bovine Serum (FBS) (Gibco, 10099141, Carlsbad, CA, USA) and 1% penicillin/streptomycin (Abiowell, AWH0529a, Changsha, China). The cells were maintained at 37°C with 5% CO_2.

Experimental grouping

In the initial experiment, cells were assigned to 5 groups: 1. Control: Cells were grown in a medium with glucose (5.5 mM) and mannitol (27.5 mM) for 24 h. 2. HG: Cells were grown in a medium with glucose (33 mM) for 24 h. 3. HG + Diosgenin (Selleck, S2291, Houston, TX, USA) 10 μg/mL: Cells were grown in a medium with glucose (33 mM) and 10 μg/mL Diosgenin for 24 h. 4. HG + Diosgenin 50 μg/mL: Cells were grown in a medium with glucose (33 mM) and 50 μg/mL Diosgenin for 24 h. 5. HG + Diosgenin 100 μg/mL: Cells were cultivated in a medium with glucose (33 mM) and 100 μg/mL Diosgenin for 24 h.

During the second experiment, cells were categorized into 5 groups: 1. HG: Cells were grown in a medium with glucose (33 mM) for 24 h. 2. HG + oe-NC: After transfecting cells with oe-NC, they were cultivated in a medium with glucose (33 mM) for 24 h. 3. HG + oe-Nrf2: After transfecting cells with oe-Nrf2, they were grown in a medium with glucose (33 mM) for 24 h. 4. HG + oe-Nrf2 + oe-NC: Cells were grown in a medium with glucose (33 mM) for 24 h after transfecting them with oe-Nrf2 and oe-NC. 5. HG + oe-Nrf2 + oe-NLRP3: Cells were grown in a medium with glucose (33 mM) for 24 h after transfecting them with oe-Nrf2 and oe-NLRP3.

In the third experiment, cells were divided into 5 groups: 1. Control: Cells were cultivated in a medium with glucose (5.5 mM) and mannitol (27.5 mM) for 24 h. 2. HG: Cells were grown in a medium with glucose (33 mM) for 24 h. 3. Diosgenin: Cells were cultivated in a medium with Diosgenin (100 μg/mL) and glucose (33 mM) for 24 h. 4. Diosgenin + si-NC: Cells were transfected with sh-NC and cultivated in a medium with Diosgenin (100 μg/mL) and glucose (33 mM) for 24 h. 5. Diosgenin + si-Nrf2: Cells were grown in a medium with glucose (33 mM) and

Diosgenin (100 μg/mL) for 24 h after transfecting them with sh-Nrf2 interference plasmids.

Cell transfection

The required transfection plasmid was thawed. Centrifuge tubes were filled with 95 μL of serum-free RPMI 1640 medium (Abiowell, AW-M018, Changsha, China). Next, 3 μg transfection plasmid and 5 μL Lipofectamine 2000 (Invitrogen, 11668019, Carlsbad, CA, USA) were introduced into the centrifuge tubes. The sequence of si-Nfr2 plasmid (Honorgene, HG-SM010902, Changsha, China) was GGACTATGAGCTGGAAAAACA. The sequence of the oe-Nrf2 plasmid (Honorgene, HG-OM010902, Changsha, China) was GATGGACTTGGAGTTGCCAC. The sequence of oe-NLRP3 plasmid (Honorgene, HG-OH145827, Changsha, China) was CGAGTGTGTCCG.

High-Performance Liquid Chromatography-mass spectrometry (HPLC-MS)

Diosgenin in HeShenwan was assessed by HPLC-MS employing QTRAP MS (SCIEX, QTRAP 5500) interfaced with a UPLC system (SCIEX, ExionLC AD). HeShenwan was loaded onto a T3 column (Waters, Milford, MA, USA, 2.1 × 100 mm, 1.7 μm particle size) maintained at a column temperature of 40°C. The mass spectrometer was run on a Turbo V ion source in negative mode. Metabolites were detected in single ion monitoring mode, optimized for declustering potentials and collision energies.

Cell counting Kit-8 (CCK-8) assay

300 μL of media was included in each well of a 96-well plate, resulting in a cell density of 5×10^3 per well. The plate was then returned to the incubator for cultivation. Following treatment according to the above method for the specified time, each well received an addition of the medium containing 10% CCK8 working solution (AWC0114b, Abiowell). After a 4-h incubation, the optical density (OD) at 450 nm was determined with a microplate reader (Heales, MB-530, Shenzhen, China).

Flow cytometry

Cells from each group were harvested using trypsin (Abiowell, AWC0232, Changsha, China) without Ethylene diamine tetraacetic acid (EDTA). The supernatant was disposed of following a 5-min centrifugation at 400 g. The cells underwent 2 rounds of Phosphate Buffered Saline (PBS) washing before being centrifuged for 5 min at 2000 rpm using a centrifuge (Zhixinlab, SL02, Shanghai, China). The cell pellet was then extracted and reconstituted in FAM-YVAD-FMK (AAT Bioquest, AAT-13483, Sunnyvale, CA, USA) (Caspase-1 working solution) for labeling Caspase-1. The cells were treated with antibodies for 1 h away from light. Subsequently, the cells were analyzed using a flow cytometer (Beckman, A00-1-1102, Brea, CA, USA).

Biochemical detection

The supernatant (500 μL) of each group of cell cultures was taken and centrifuged at 6000 rpm for 5–10 min at 4°C using a centrifuge (Zhixinlab, SL02, Shanghai, China), and then the supernatant was collected. SOD content was detected by the SOD test kit (Njjcbio, A001-3, Nanjing, China), and MDA levels were detected by the MDA assay kit (Njjcbio, A003-1, Nanjing, China).

Enzyme-linked immunosorbent assay (ELISA)

Each group of cells was gathered, and after 15 min at 2°C–8°C and 1000 g of centrifugation, the supernatant was extracted. IL-1β, IL-18, LDH and HMGB1 levels were measured according to the instructions of IL-1β (Cusabio, CSB-E08054m, Wuhan, China), IL-18 (Cusabio, CSB-E08054m, Wuhan, China), LDH (Njjcbio, A020-2, Nanjing, China) and HMGB1 (Cusabio, CSB-E08225m, Wuhan, China) ELISA kits, respectively.

ROS content detection

DCFH-DA (Amresco, D1002, Washington, DC, USA) was diluted to 10 μM in a serum-free culture medium. After removing the cell culture supernatant from each group of cells, DCFH-DA was added in the appropriate amount. After that, the cells were cultivated for 20 min at 37°C. The cells were then taken from each group, cleaned 3 times, and subjected to flow cytometry analysis.

Western blot

The cells were gathered and cleaned with pre-cooled PBS buffer, and RIPA lysate (AWB0136, Abiowell) was added in proportion to lyse the cells. Protein concentration was measured using a BCA kit (AWB0156, Abiowell). Protein samples of equal volumes were combined with 5 × loading buffer (AWB0055, Abiowell) and boiled for 5 min to denature the proteins. When the bromophenol blue electrophoresis reached the gel's bottom, the electrophoresis was stopped. The gel was cut according to the molecular weight, and 6 pieces of filter paper and 1 piece of NC membrane (Beijing Biolab-Tech, QN1171, Beijing, China) of the same size as the gel were prepared. The NC membrane and the filter paper were put into the transfer buffer solution together until they were completely immersed. Put the filter paper and NC membrane in order. Cover the instrument, turn on the power supply, and 300 mA constant current transfer film. The film current was 300 mA, and the transfer time was adjusted according to different antibodies. After the membrane was transferred, the membrane was rinsed once in 1 × PBST (Abiowell, AWI0130, Changsha, China), and then the blocking solution submerged the membrane entirely. On a shaker, the membrane was shaken for 90 min at room temperature. Primary antibodies were diluted using 1 × PBST in a ratio of NLRP3 (Abiowell, AWA46822, 1:1000, Changsha, China), ASC (Abiowell, AWA44043, 1:1000, Changsha, China), GSDMD (Proteintech, 20770-1-AP, 1:5000, San Diego, CA, USA), Caspase-1 (Proteintech, 22915-1-AP, 1:6000, San Diego, CA, USA), Nrf2 (Abiowell, AWA48931, 1:1000, Changsha, China), β-actin (Abiowell, AWA80002, 1:5000, Changsha, China). The membranes were treated with primary antibodies, which were then left overnight at 4°C. The membranes were left at room temperature for 30 min the next day. The membranes were then treated with diluted secondary antibodies Goat anti-Mouse IgG (H + L) (Abiowell, AWS0001, 1:5000, Changsha, China), Goat anti-Rabbit IgG (H + L) (Abiowell, AWS0002, 1:5000, Changsha, China,), HRP goat anti-rabbit IgG

(Proteintech, SA00001-2, 1:6000, San Diego, CA, USA) for 90 min at room temperature after the incubation time. The results were seen using a chemiluminescence imaging system (Clinx Science Instruments, ChemiScope6100, Shanghai, China). Software called ImageJ (1.52 V) (National Institutes of Health, Bethesda, MD, USA) was used to examine the outcomes.

Molecular dynamics simulation

The experiment was conducted using the software GROMACS 2023 (Uppsala University, SE) for molecular dynamics simulation. Unrestrained molecular dynamics simulations of the molecular docking complex of Diosgenin and Nrf2 were performed using the Charmm36 force field and TIP3P water model. In brief, the mol2 format file of Diosgenin was uploaded to the CGenFF server (https://cgenff.umaryland.edu/initguess/, accessed on 10 May 2024) to generate the corresponding 'str' file. Subsequently, the python2.7 executable script cgenff_charmm2gmx.py (http://mackerell.umaryland.edu/charmm_ff.shtml#gromacs, accessed on 10 May 2024), corresponding to the Charmm36 force field was used to convert the molecular topology file into a format recognizable by the Charmm36 force field. The simulation systems were all solvated in cubic solvent boxes, and periodic boundary conditions of 1 nm were applied. Initially, 500 ps of NVT and 1000 ps of NPT equilibration were conducted to stabilize the system. The temperature and pressure of the system were controlled to reach 310 K and 1 bar, respectively. Finally, a 100 ns molecular dynamics simulation was performed on the complex.

Reverse transcription-quantitative polymerase chain reaction (RT-qPCR)

Using Trizol (Thermo, 15596026, Waltham, MA, USA), total RNA was extracted from cultivated cells. UV spectrophotometry was then used to determine the concentration and purity of the extracted material. A reverse transcription kit (Cwbio, CW2569, Taizhou, China) was used to create cDNA. Using UltraSYBR Mixture (Cwbio, CW2601, Taizhou, China) and the $2^{-\Delta\Delta Ct}$ technique for gene expression analysis, β-actin was used as the internal control. Primer sequences were: M-β-actin: F: 5′-ACA TCCGTAAAGACCTCTATGCC-3′, R: 5′-TA CTCCTGCTTGCTGATCCAC-3′.

M-NLRP3: F: 5′-CCTCTTTGGCCTTGTAAACCAG-3′, R: 5′-TGGCTTTCACTTCAATCCACT-3′. M-Nrf2: F: 5′-GCTCCTATGCGTGAATCCCAA-3′, R: 5′-TTTGCCCTAA GCTCATCTCGT-3′.

Statistical analysis

GraphPad Prism 8.0.1 (Graphpad Software Inc., San Diego, CA, USA) was used to do statistical analysis, and all data were presented as mean ± standard deviation (SD). For samples that were normally distributed, comparisons between two groups were performed using *t*-tests, comparisons among multiple groups were performed using one-way ANOVA, and *post hoc* multiple comparisons were conducted using Tukey's multiple comparisons test. $p < 0.05$ was considered statistically significant. Each assay was repeated three times during the statistical analysis.

Results

HPLC-MS was used to detect the chemical components of the HeShenwan

To determine the chemical composition of HeShenwan, we conducted an HPLC-MS analysis. The results showed that HeShenwan contained a variety of components, among which Diosgenin had the highest content (Fig. 1).

Diosgenin ameliorated HG-induced oxidative stress and pyroptosis in podocytes

To study the effects of Diosgenin on HG-induced podocytes, HG-induced mpc5 cells were used to create a podocyte injury model. The HG group cell viability was much lower than the Control group. In contrast to the HG group, the cell viability considerably increased in the HG + Diosgenin 10 μg/mL, HG + Diosgenin 50 μg/mL, and HG + Diosgenin 100 μg/mL groups (Fig. 2A). Flow cytometry results, as shown in Fig. 2B, the pyroptosis rate of HG treated cells increased remarkably. However, the rate of pyroptosis noticeably decreased in the HG + Diosgenin 10 μg/mL, HG + Diosgenin 50 μg/mL, and HG + Diosgenin 100 μg/mL groups compared to the HG group. These results suggest that Diosgenin can ameliorate HG-induced mpc5 cell injury and pyroptosis, exhibiting a dose-dependent relationship within a certain concentration range. The SOD and the MDA content increased significantly in the HG group compared to the Control group. However, after adding Diosgenin at different concentrations (10, 50, and 100 μg/mL), the SOD content significantly increased, and the MDA content markedly decreased (Fig. 2C,D). Comparing the HG group to the Control group, there is an important increase in IL-1β, IL-18, LDH, and HMGB1 levels. On the other hand, these levels significantly decreased when Diosgenin (10, 50, and 100 μg/mL) was added (Fig. 2E–G). The ROS level was significantly increased after HG intervention, but they dramatically dropped when different quantities of Diosgenin (10, 50, and 100 μg/mL) were added (Fig. 2H). The HG group had considerably higher expression levels of NLRP3, Caspase-1, GSDMD, and ASC than the Control group did. In contrast, the groups treated with Diosgenin at varying concentrations (10, 50, and 100 μg/mL) showed significantly lower expression levels of these genes than in the HG group (Fig. 2I). These results suggest that Diosgenin could mitigate oxidative stress and pyroptosis in podocytes induced by HG, demonstrating a dose-dependent relationship within a specific concentration range.

Diosgenin regulated the expression of Nrf2

One of the therapeutic targets for DKD, Nrf2, is crucial for the regulation of cellular oxidative stress. It functions as a highly sensitive signal for removing intracellular ROS to combat oxidative stress [19]. To further explore how Diosgenin alleviated oxidative stress and pyroptosis in mpc5 cells, we obtained the molecular structure of Diosgenin from the

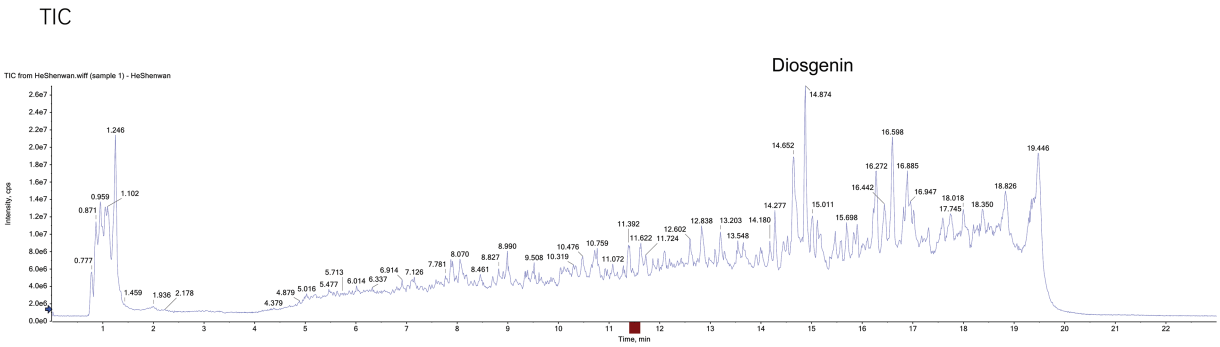

FIGURE 1. HPLC-MS detected the chemical components of HeShenwan.

Pubmed (https://pubmed.ncbi.nlm.nih.gov/, accessed on 10 May 2024) compound (Fig. 3A). We performed molecular docking between the molecular structure of Diosgenin and the Nrf2 protein. The molecular docking results are shown in Fig. 3B–D. The binding energy of this molecular docking was −11.9 kcal/mol. Since the binding energy was below −5 kcal/mol, it suggested that Diosgenin could spontaneously bind well to the Nrf2 protein. Through visual analysis using PYMOL (Schrödinger, Inc., New York, NY, USA), it was observed that Diosgenin could stably bind to the cavity of the Nrf2 protein and interact with the surrounding amino acids. Diosgenin primarily interacted with the Nrf2 protein through hydrogen bonding and hydrophobic interactions. Diosgenin could form stable

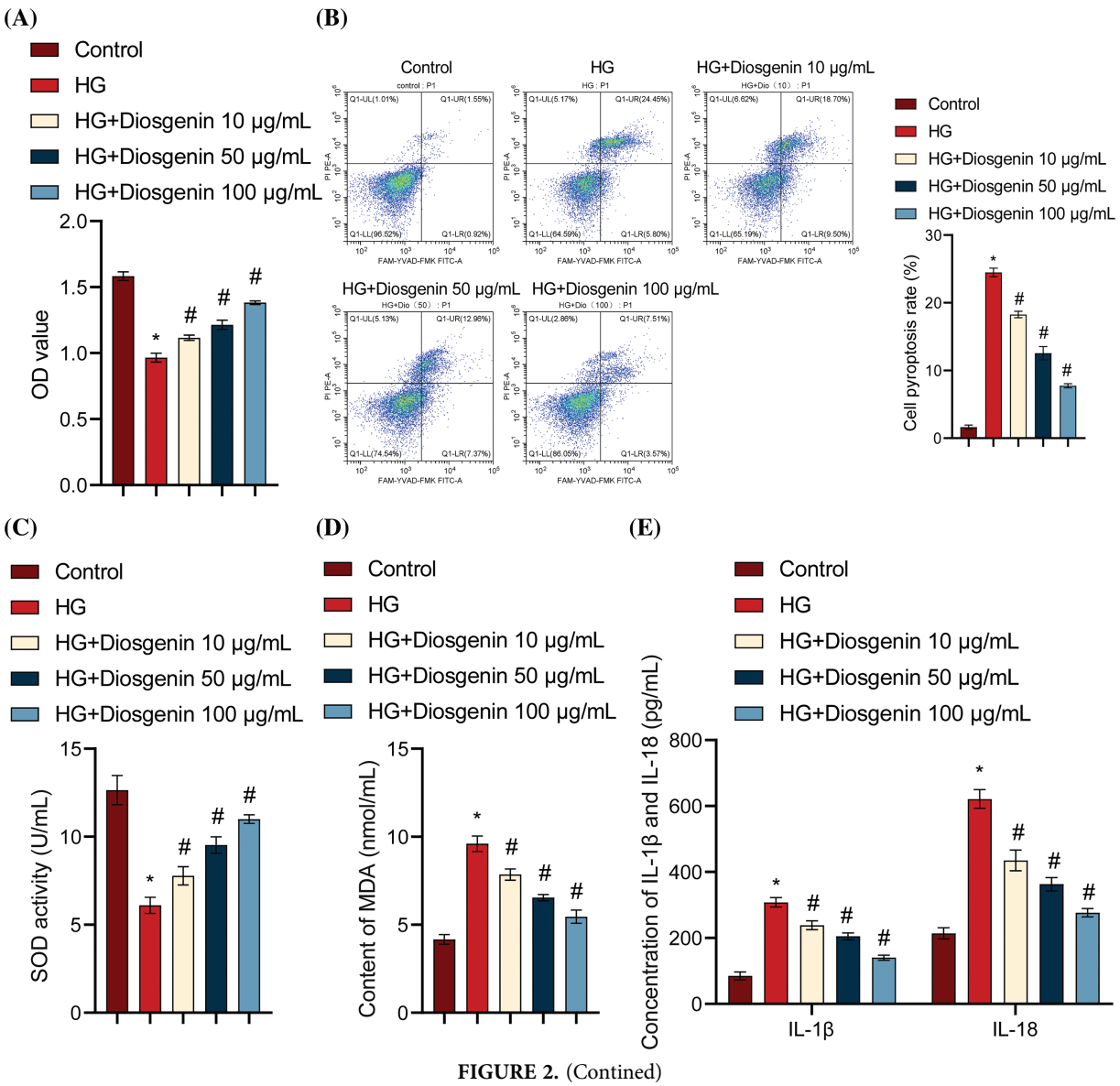

FIGURE 2. (Contined)

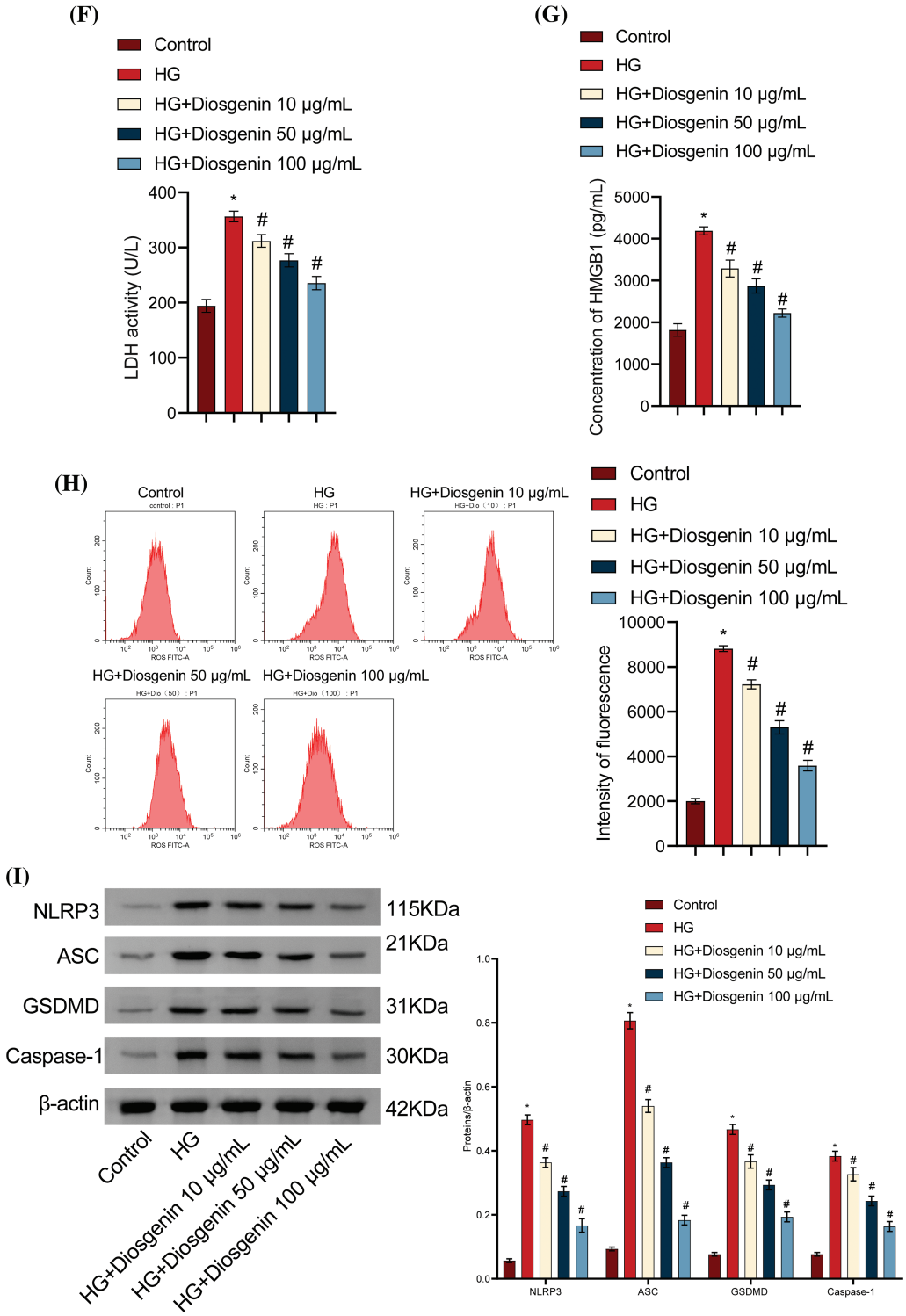

FIGURE 2. Diosgenin ameliorated HG-induced oxidative stress and pyroptosis in podocytes. (A) mpc5 cell viability was assessed using CCK-8 assay. (B) Pyroptosis in mpc5 cells was evaluated by flow cytometry. (C and D) SOD and MDA levels were measured through biochemical analysis. (E–G) The levels of IL-1β, IL-18, LDH, and HMGB1 were detected by ELISA. (H) The ROS content was assessed using flow cytometry. (I) NLRP3 and pyroptosis-related indicators Caspase-1, GSDMD, and ASC expression were examined using Western blot analysis. $^{*}p < 0.05$ *vs*. Control, $^{\#}p < 0.05$ *vs*. HG, n = 3.

hydrogen bonds with ARG 415 in the Nrf2 protein; the hydrophobic groups in Diosgenin could interact with ALA 366 and VAL 418 in the Nrf2 protein, serving as the main driving force for Diosgenin to bind to the active site. As shown in Fig. A1(A), the Root Mean Square Deviation (RMSD) value of the Nrf2-Diosgenin complex was 0.09601531 ± 0.00919304 nm, which was less than the RMSD value of free protein (0.1079431 ± 0.01025337 nm), indicating that the structure of Diosgenin and Nrf2 complex was more stable after binding. The Root Mean Square

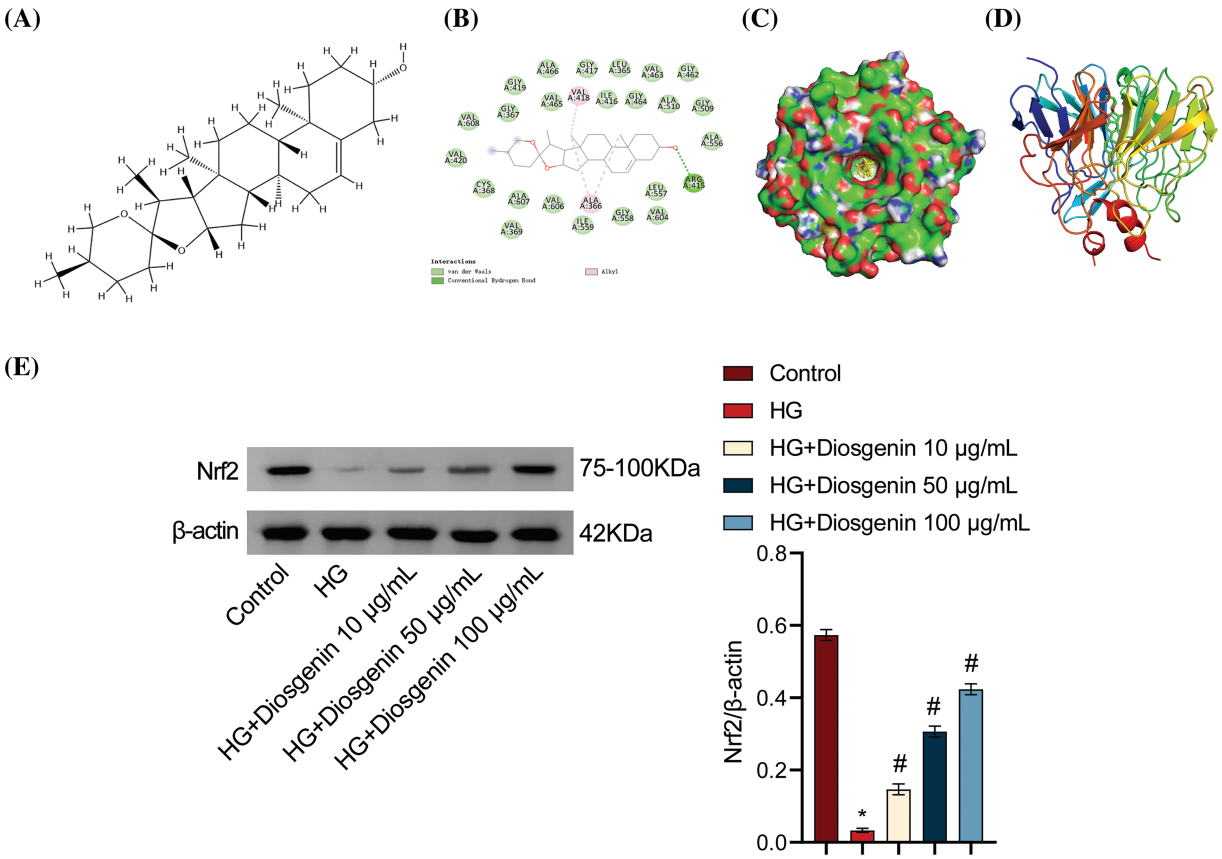

FIGURE 3. Diosgenin regulated the expression of Nrf2. (A) Chemical structure of Diosgenin. (B) Molecular docking between Diosgenin and Nrf2. (C) Surface structures formed by Diosgenin around the active center of Nrf2. (D) Diagram of Diosgenin-Nrf2 interaction. (E) Western blot assay to measure levels of Nrf2. $^{*}p < 0.05$ *vs.* control, $^{\#}p < 0.05$ *vs.* HG, n = 3.

Fluctuation (RMSF) value of the Nrf2-Diosgenin complex was 0.09434371 ± 0.04937059 nm, which was slightly higher than the RMSF value of free protein (0.09423427 ± 0.04943270 nm) (Fig. A1(B)). Fig. A1(C) showed that the radiuses of gyration (Rg) value of Nrf2-Diosgenin complex (1.801415 ± 0.006693535 nm) was slightly higher as compared to that of free protein (1.797737 ± 0.006030057 nm). The main protease of Nrf2-Diosgenin complex had the solvent accessible surface area (SASA) value of 126.5466 ± 2.159216 nm^2, which was slightly higher compared to the average SASA value of free protein (126.2392 ± 1.858181 nm^2) (Fig. A1(D)). These results showed that the structural stability of the Nrf2-Diosgenin complex was not much different from that of free protein. The Western blot analysis results indicated that Nrf2 expression in the HG group was markedly lower compared to the Control group. Conversely, Nrf2 expression levels were significantly increased in the HG + Diosgenin 10 μg/mL, HG + Diosgenin 50 μg/mL, and HG + Diosgenin 100 μg/mL groups compared to the HG group (Fig. 3E). These findings suggested that Diosgenin may control Nrf2 expression.

Nrf2-mediated antioxidant pathway inhibited HG-induced podocyte pyroptosis by affecting NLRP3 activation

The previous results demonstrated that Diosgenin could improve oxidative stress and pyroptosis in HG-induced mpc5 cells and could also regulate the expression of Nrf2. Additionally, NLRP3 played a significant role in pyroptosis [20]. To explore the relationship between Nrf2 and NLRP3, we set up Nrf2 and NLRP3 overexpression groups. As seen in Fig. 4A,B, there was a noteworthy rise in Nrf2 levels in the HG + oe-Nrf2 group relative to the HG + oe-NC group. Compared to the HG + oe-Nrf2 + oe-NC group, there was no discernible change in Nrf2 expression in the HG + oe-Nrf2 + oe-NLRP3 group, indicating that NLRP3 overexpression did not impact Nrf2 expression. Furthermore, after transfection with oe-Nrf2, the expression of NLRP3 significantly decreased, indicating that Nrf2 overexpression was the cause of the drop in NLRP3 expression. Cell viability was significantly increased after transfection with oe-Nrf2, and cell viability further decreased when transfected with oe-NLRP3 (Fig. 4C). The pyroptosis rate was significantly lower in the HG + oe-Nrf2 group as compared to the HG + oe-NC group, according to the flow cytometry results displayed in Fig. 4D. In contrast, the pyroptosis rate in the HG + oe-Nrf2 + oe-NLRP3 group was significantly higher than the HG + oe-Nrf2 + oe-NC group. This finding suggests that the overexpression of Nrf2 reduces NLRP3 expression, thereby alleviating damage and pyroptosis in mpc5 cells induced by HG. SOD and MDA measurements revealed that SOD content was significantly increased and MDA content was significantly decreased after transfection with oe-Nrf2. In contrast to the HG + oe-Nrf2 + oe-NC group, the SOD content significantly dropped, and the MDA content rose in the HG + oe-Nrf2 + oe-NLRP3 group (Fig. 4E,F). ELISA results showed that the

levels of IL-1β, IL-18, LDH, and HMGB1 were significantly decreased after transfection with oe-Nrf2. On the other hand, the levels in the HG + oe-Nrf2 + oe-NLRP3 group were considerably higher than those in the HG + oe-Nrf2 + oe-NC group (Fig. 4G–I). The results of ROS level detection are shown in Fig. 4J. The intracellular ROS content was significantly decreased after transfection with oe-Nrf2. In contrast, the HG + oe-Nrf2 + oe-NLRP3 group had a considerably greater ROS content than the HG + oe-Nrf2 + oe-NC group. Western blot results showed that the expression levels of NLRP3, Caspase-1, GSDMD, and ASC were significantly decreased after transfection with oe-Nrf2. Additionally, compared to the HG + oe-Nrf2 + oe-NC group, the expression levels were significantly greater in the HG + oe-Nrf2 + oe-NLRP3 group (Fig. 4K). In conclusion, these results demonstrate that Nrf2 reduces oxidative stress and inhibits HG-induced podocyte pyroptosis by affecting the activation of NLRP3.

Diosgenin inhibited HG-induced podocyte pyroptosis via the Nrf2/NLRP3 axis

To determine the specific role of Diosgenin in inhibiting HG-induced podocyte apoptosis, we knocked down Nrf2 and performed Western blot and RT-qPCR assays. The findings presented in Fig. 5A,B indicated that the level of Nrf2 in the si-NC group did not substantially differ from that of the Control group. The Nrf2 level in the si-Nrf2 group considerably decreased when compared to the si-NC group, suggesting an effective knockdown of Nrf2. The cell viability in the Diosgenin group was much higher than in the HG group, it decreased in the HG group as compared to the Control group. When compared to the Diosgenin + si-NC

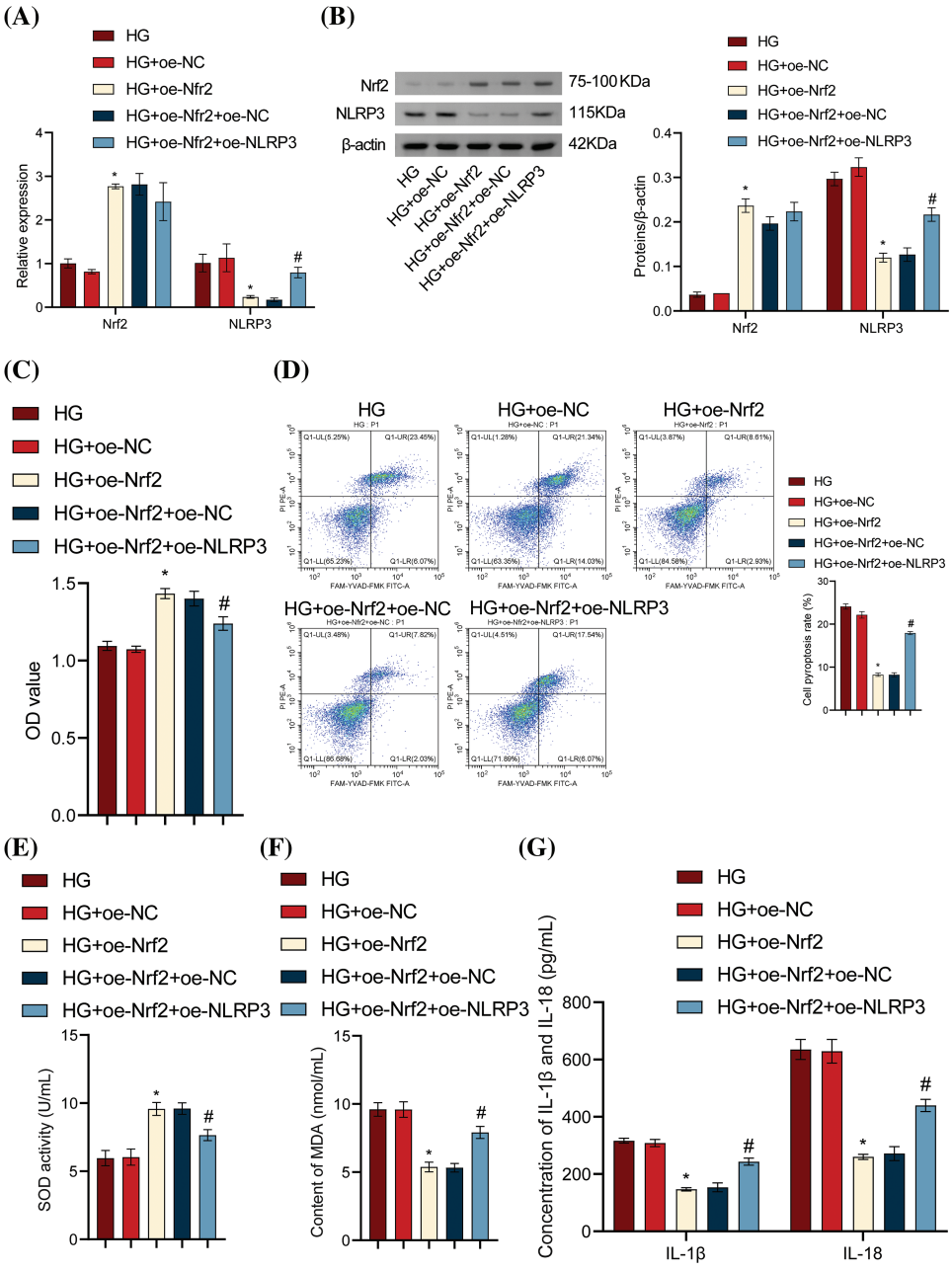

FIGURE 4. (Contined)

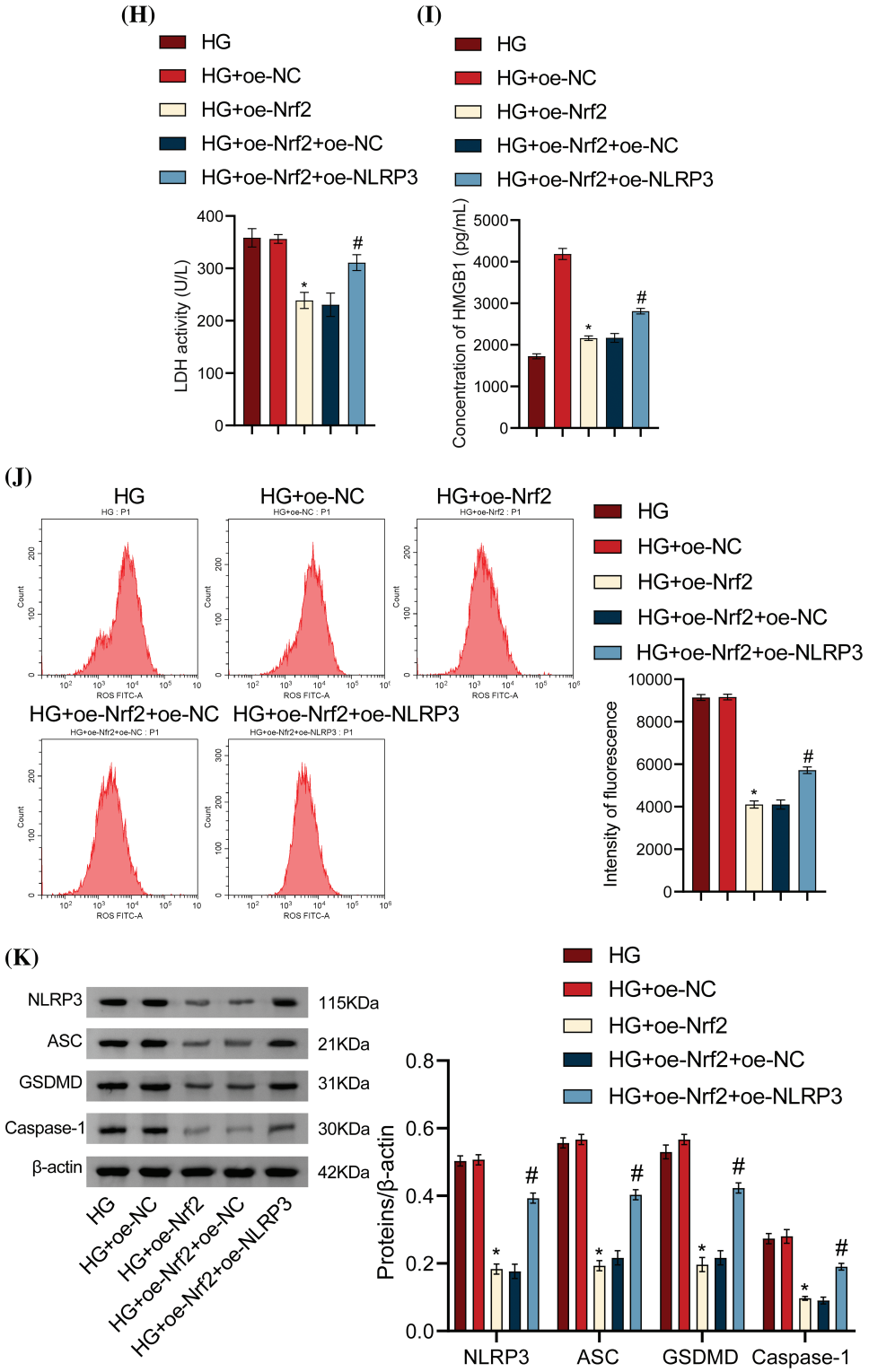

FIGURE 4. Nrf2-mediated antioxidant pathway inhibited HG-induced podocyte pyroptosis by affecting NLRP3 activation. (A) Nrf2 and NLRP3 levels were measured using RT-qPCR. (B) Nrf2 and NLRP3 levels were determined by Western blot analysis. (C) Cell viability of mpc5 cells was assessed with the CCK-8 assay. (D) Pyroptosis of mpc5 cells was analyzed using flow cytometry. (E and F) Biochemical analysis was conducted to measure the content of SOD and MDA. (G–I) IL-1β, IL-18, LDH, and HMGB1 levels were determined by ELISA. (J) ROS content was assessed using flow cytometry. (K) The levels of NLRP3 and pyroptosis-related indicators Caspase-1, GSDMD, and ASC were detected by the Western blot assay. $^{*}p < 0.05$ *vs.* HG + oe-NC, $^{\#}p < 0.05$ *vs.* HG + oe-Nrf2 + oe-NC, n = 3.

group, the cell viability in the Diosgenin + si-Nrf2 group dramatically dropped (Fig. 5C). The pyroptosis rate of cells in the Diosgenin group was remarkably lower than in the HG group, according to the flow cytometry results in Fig. 5D. At the same time, it was remarkably higher in the Diosgenin + si-Nrf2 group than the Diosgenin + si-NC

group. This finding suggests that Nrf2 knockdown reduces Diosgenin's ability to improve HG-induced damage and apoptosis in mpc5 cells. The findings of the SOD and MDA assays showed that the Diosgenin group had significantly higher SOD content and lower MDA content than the HG group. In contrast, when comparing the Diosgenin + si-Nrf2 group to the Diosgenin + si-NC group, the SOD content dramatically dropped, and the MDA content significantly increased (Fig. 5E,F). The Diosgenin group had considerably lower levels of IL-1β, IL-18, LDH, HMGB1, and ROS than the HG group, according to the results of the ELISA and ROS assay. On the other hand, the Diosgenin + si-Nrf2 group exhibited a significant rise in HMGB1, ROS, LDH, IL-1β, and IL-18 levels in comparison to the Diosgenin + si-NC group (Fig. 5G–J). The Western blot results in Fig. 5K revealed that in comparison to the HG group, Nrf2 expression increased in the Diosgenin group, NLRP3, Caspase-1, GSDMD, and ASC expressions declined. The Diosgenin + si-Nrf2 group displayed higher expressions of NLRP3, Caspase-1, GSDMD, and ASC and decreased expression of Nrf2 in comparison to the Diosgenin + si-NC group. Previous research has indicated that Diosgenin can modulate Nrf2 expression, and Nrf2 can impact NLRP3 activation. These results prove that Diosgenin inhibited HG-induced apoptosis in mpc5 cells through the Nrf2/NLRP3 axis.

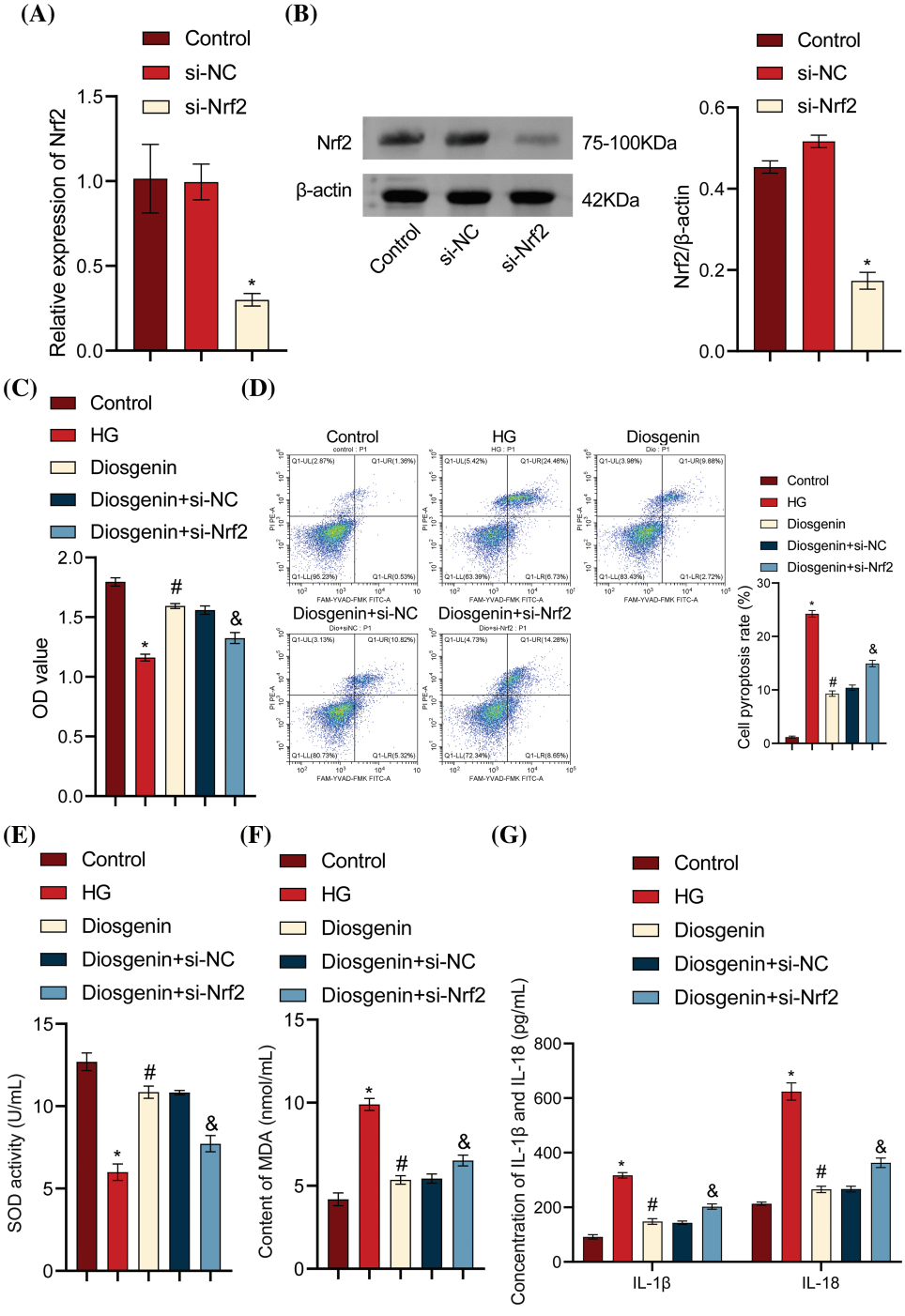

FIGURE 5. (Contined)

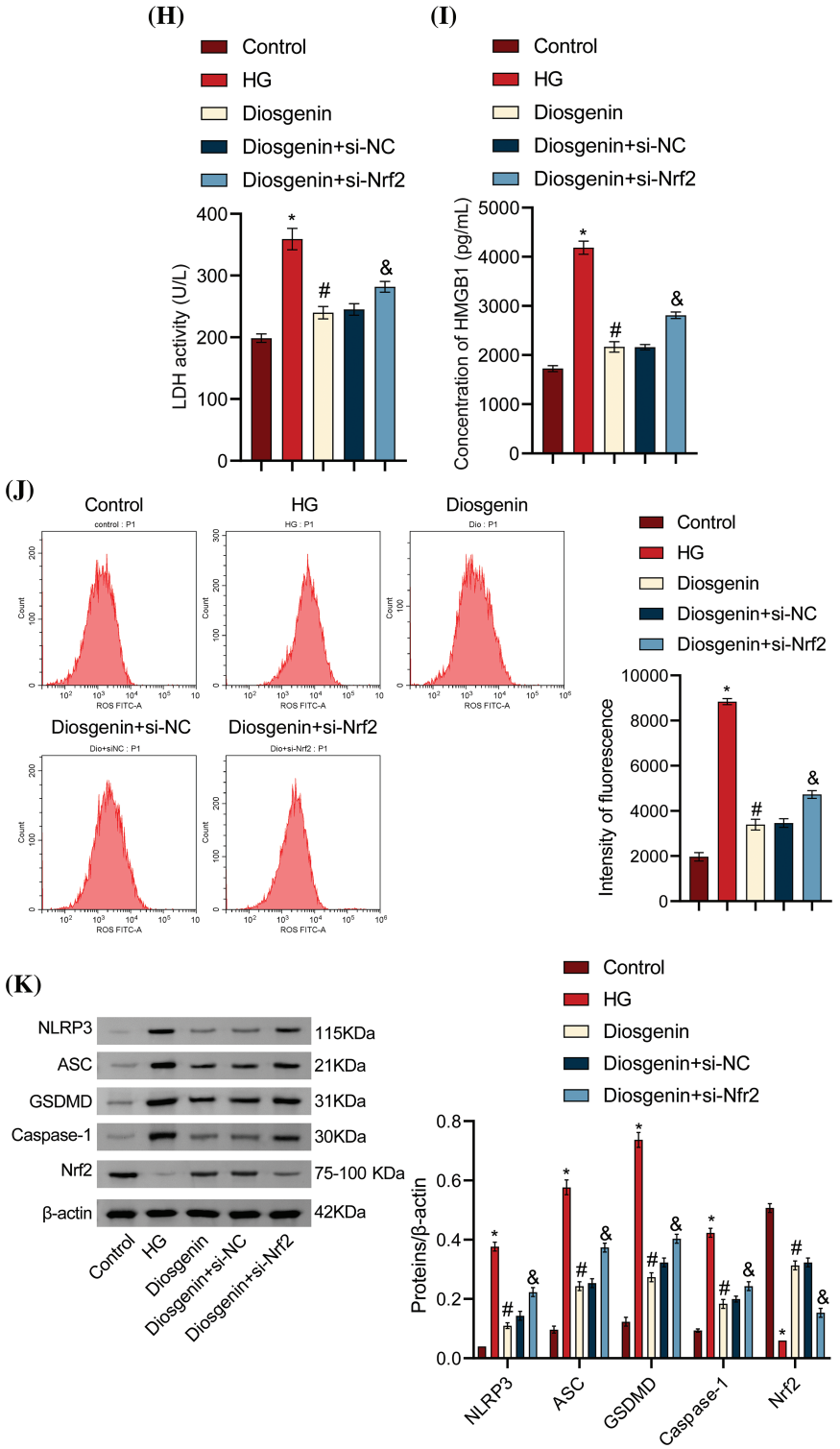

FIGURE 5. Diosgenin inhibited HG-induced podocyte pyroptosis via the Nrf2/NLRP3 axis. (A) Nrf2 levels were measured by RT-qPCR. (B) Nrf2 levels were detected by the Western blot assay. (C) Cell viability of mpc5 cells was assessed by CCK-8 assay. (D) Pyroptosis of mpc5 cells was analyzed using flow cytometry. (E and F) Biochemical analysis was conducted to measure the content of SOD and MDA. (G–I) Levels of IL-1β, IL-18, LDH, and HMGB1 were detected by ELISA. (J) The ROS content was assessed using flow cytometry. (K) The expression of NLRP3 and pyroptosis-related indicators Caspase-1, GSDMD, and ASC was detected by the Western blot assay. $^{*}p < 0.05$ *vs.* Control, $^{\#}p < 0.05$ *vs.* HG, $^{\&}p < 0.05$ *vs.* Diosgenin + si-NC, n = 3.

Discussion

DKD, a common diabetes complication, accounts for 30% to 50% of end-stage renal disease and has become a serious public health issue threatening the health of people worldwide [21]. In clinical practice, the extent of podocyte injury was commonly utilized as an indicator to assess the progression and severity of DKD [22,23]. Therefore, the

treatment aimed at protecting podocytes was considered to be of significant importance in the management of DKD. However, the exact mechanism of podocyte injury and death in DKD remained unclear. The research on regulating the Nrf2/NLRP3 pathway to inhibit podocyte pyroptosis for the treatment of DKD was innovative. This study comprehensively investigated the molecular mechanisms of this pathway through experimental data obtained from cell experiments.

Diosgenin was a natural steroidal saponin obtained from plants of the Solanum and Dioscorea genera, and it was involved in the synthesis of steroid hormones. As a key ingredient for manufacturing steroid medications, it has multiple pharmacological effects and has been proven to successfully treat cardiovascular diseases, neurodegenerative diseases, and DKD [23–25]. Currently, research on Diosgenin in DKD is still in the early stages, and its potential targets and pharmacological mechanisms await further investigation. In this work, HG induction was used to create an mpc5 cell damage model, and varying concentrations of Diosgenin (10, 50, and 100 μg/mL) were introduced to the impaired cells for intervention. The results showed that all 3 concentrations of Diosgenin could reduce oxidative stress and pyroptosis in mpc5 cells by HG to varying degrees. Research by Zhong et al. [26] has shown that Diosgenin could reduce ROS production and cell apoptosis to mitigate DKD. These findings align with the outcomes of the current study, suggesting that Diosgenin could be pivotal in DKD treatment.

Being a pivotal transcription factor in oxidative stress regulation, Nrf2 performs essential functions in triggering the body's antioxidant response [27,28]. Previous studies have shown that Nrf2 can resist DKD by inhibiting oxidative stress and inflammation [29]. In this study, Diosgenin was found to form a stable hydrogen bond with the ARG 415 of the Nrf2 protein, and the hydrophobic groups of Diosgenin could interact hydrophobically with the ALA 366 and VAL 418 of the Nrf2 protein. These interactions could promote the binding of Diosgenin to the Nrf2 protein and regulate the expression of the Nrf2 protein. This research finding was innovative and suggested that Diosgenin may achieve its therapeutic effects in treating DKD by regulating the Nrf2 protein.

NLRP3 inflammatory vesicles were a critical component of the intrinsic immune system, and their activation induced rapid release of interleukin IL-1β and response to exogenous or endogenous danger signals by inducing Caspase-1 molecule activation and programmed cell death [30,31]. In a study by Zu et al. icariin inhibited osteoarthritis by suppressing NLRP3/Caspase-1 signaling-mediated pyroptosis [32]. Xiao's research demonstrated that stimulator of interferon genes (STING) increased hepatocyte pyroptosis mediated by NLPR3 and NLRP3 inflammasomes through the interferon regulatory transcription factor 3/WD repeat-containing protein 5/DOT1-like histone H3K79 methyltransferase (IRF3/WDR5/DOT1L) transcriptional activation complex in epigenetic regulation. Inhibiting the STING-NLRP3-GSDMD signaling pathway could protect hepatocytes from pyroptosis and alleviate liver inflammation and fibrosis [33]. In this study, an NLRP3 overexpression group was constructed, and the results indicated that upregulating NLRP3 expression increased pyroptosis in mpc5 cells, confirming the crucial role of NLRP3 in pyroptosis. Research has demonstrated that Nrf2 can reduce cellular damage from oxidative stress by regulating the intracellular antioxidant defense system, thereby inhibiting pyroptosis to some extent and playing a vital role in maintaining cell homeostasis and protecting cell health during the process of pyroptosis [34,35]. Whether there is a regulatory relationship between Nrf2 and NLRP3 is unknown. This study demonstrated through overexpression studies that the expression of NLRP3 did not affect the levels of Nrf2, while overexpression of Nrf2 reduced the levels of NLRP3, Nrf2 mediated antioxidant by affecting NLRP3 activation to inhibit HG-induced pyroptosis in mpc5 cells. The mechanism by which ellagic acid alleviates gouty arthritis in the study by Lin et al. [36] is consistent with this study, as it involves enhancing the Nrf2 signal to inhibit NLRP3 inflammasome activation and pyroptosis.

We have demonstrated that Diosgenin interacted with the Nrf2 protein and regulated its expression. Nrf2 influenced the activation of NLRP3 to mediate antioxidation, thereby inhibiting pyroptosis in HG-induced mpc5 cells. Whether diosgenin can inhibit HG-induced pyroptosis in mpc5 cells by modulating the Nrf2/NLRP3 pathway is unknown. This study further conducted Nrf2 knockdown experiments and measured pyroptosis-related indicators, and findings verified that Diosgenin could regulate the Nrf2/NLRP3 axis, which would prevent pyroptosis in mpc5 cells induced by HG.

However, our study still has several limitations. Firstly, in studying the binding of Diosgenin with Nrf2, due to the lack of specialized software for molecular dynamics analysis, we only used PYMOL for visual analysis and did not conduct a molecular dynamics simulation of the binding between Diosgenin and Nrf2. Following that, abnormal levels of Nrf2 may result in DNA damage within cells [37], but this study primarily focused on the regulation of the Nrf2/NLRP3 pathway by Diosgenin, without investigating the impact of Diosgenin on the central rule of DNA polymorphism from 5′-3′ to 3′-5′ while regulating the Nrf2 pathway. Additionally, our study only confirmed that Diosgenin could inhibit HG-induced DKD cell pyroptosis by modulating the Nrf2/NLRP3 pathway at the cellular level. However, due to financial constraints, animal experiments have not yet been conducted to further investigate the impact of Diosgenin on DKD. These are also aspects that we plan to further explore in our future research, aiming to enrich the theoretical basis for Diosgenin in treating DKD.

In conclusion, our study provided evidence that via modifying the Nrf2/NLRP3 pathway, Diosgenin could prevent pyroptosis in HG-induced mpc5 cells. These results imply that Diosgenin could be a promising approach for treating DKD, offering a new therapeutic strategy to enhance treatment options for patients with DKD.

Acknowledgement: None.

Funding Statement: This work was supported by the General Funded Project of Hunan Provincial Health Commission (No.

202203054238), the Hunan University of Chinese Medicine Campus Joint Fund Project (Nos. 2023XYLH022, 2023XYLH028), the Project of Key Specialties of Chinese Medicine in Hunan Province (czxm-sbk-2023001, czxm-nfmnk-2023001).

Author Contributions: The authors confirm their contribution to the paper as follows: Study conception, design, drafting, and revision of the manuscript: Yu Tang and Wenxiao Hu; Performed the experiments, performed the statistical analyses, and drafted the manuscript: Yajun Peng and Xiangdong Ling. All authors reviewed the results and approved the final version of the manuscript.

Availability of Data and Materials: The datasets used and analyzed during the current study are available from the corresponding author upon reasonable request.

Ethics Approval: Not applicable.

Conflicts of Interest: The authors declare that they have no conflicts of interest to report regarding the present study.

References

1. Tuttle KR, Agarwal R, Alpers CE, Bakris GL, Brosius FC, Kolkhof P, et al. Molecular mechanisms and therapeutic targets for diabetic kidney disease. Kidney Int. 2022;102(2):248–60.
2. Zhang JQ, Su BH, Zhang J, Guo XH. Expert consensus on early prediction and diagnosis of diabetic kidney disease. Zhonghua Nei Ke Za Zhi. 2021;60(6):522–32 (In Chinese).
3. Wilkinson TJ, McAdams-DeMarco M, Bennett PN, Wilund K. Advances in exercise therapy in predialysis chronic kidney disease, hemodialysis, peritoneal dialysis, and kidney transplantation. Curr Opin Nephrol Hypertens. 2020;29(5):471–9.
4. Alicic RZ, Rooney MT, Tuttle KR. Diabetic kidney disease: challenges, progress, and possibilities. Clin J Am Soc Nephrol. 2017;12(12):2032–45.
5. Zhang L, Wen Z, Han L, Zheng Y, Wei Y, Wang X, et al. Research progress on the pathological mechanisms of podocytes in diabetic nephropathy. J Diabetes Res. 2020;2020:7504798.
6. An X, Zhang L, Yuan Y, Wang B, Yao Q, Li L, et al. Hyperoside pre-treatment prevents glomerular basement membrane damage in diabetic nephropathy by inhibiting podocyte heparanase expression. Sci Rep. 2017;7(1):6413. doi:10.1038/s41598-017-06844-2.
7. Jiang W, Gan C, Zhou X, Yang Q, Chen D, Xiao H, et al. Klotho inhibits renal ox-LDL deposition via IGF-1R/RAC1/OLR1 signaling to ameliorate podocyte injury in diabetic kidney disease. Cardiovasc Diabetol. 2023;22(1):293. doi:10.1186/s12933-023-02025-w.
8. Zhu W, Li YY, Zeng HX, Liu XQ, Sun YT, Jiang L, et al. Carnosine alleviates podocyte injury in diabetic nephropathy by targeting caspase-1-mediated pyroptosis. Int Immunopharmacol. 2021;101:108236. doi:10.1016/j.intimp.2021.108236.
9. Gao Y, Ma Y, Xie D, Jiang H. ManNAc protects against podocyte pyroptosis via inhibiting mitochondrial damage and ROS/NLRP3 signaling pathway in diabetic kidney injury model. Int Immunopharmacol. 2022;107(1):108711. doi:10.1016/j.intimp.2022.108711.
10. Hou Y, Lin S, Qiu J, Sun W, Dong M, Xiang Y, et al. NLRP3 inflammasome negatively regulates podocyte autophagy in diabetic nephropathy. Biochem Biophys Res Commun. 2020;521(3):791–8. doi:10.1016/j.bbrc.2019.10.194.
11. Wang H, Lv D, Jiang S, Hou Q, Zhang L, Li S, et al. Complement induces podocyte pyroptosis in membranous nephropathy by mediating mitochondrial dysfunction. Cell Death Dis. 2022;13(3):281. doi:10.1038/s41419-022-04737-5.
12. Lv C, Cheng T, Zhang B, Sun K, Lu K. Triptolide protects against podocyte injury in diabetic nephropathy by activating the Nrf2/HO-1 pathway and inhibiting the NLRP3 inflammasome pathway. Ren Fail. 2023;45(1):2165103. doi:10.1080/0886022X.2023.2165103.
13. Chen Z, Zhong H, Wei J, Lin S, Zong Z, Gong F, et al. Inhibition of Nrf2/HO-1 signaling leads to increased activation of the NLRP3 inflammasome in osteoarthritis. Arthritis Res Ther. 2019;21(1):300. doi:10.1186/s13075-019-2085-6.
14. Li G, Liu C, Yang L, Feng L, Zhang S, An J, et al. Syringaresinol protects against diabetic nephropathy by inhibiting pyroptosis via NRF2-mediated antioxidant pathway. Cell Biol Toxicol. 2023;39(3):621–39. doi:10.1007/s10565-023-09790-0.
15. Wang Z, Wu Q, Wang H, Gao Y, Nie K, Tang Y, et al. Diosgenin protects against podocyte injury in early phase of diabetic nephropathy through regulating SIRT6. Phytomedicine. 2022;104:154276. doi:10.1016/j.phymed.2022.154276.
16. Zhang SZ, Liang PP, Feng YN, Yin GL, Sun FC, Ma CQ, et al. Therapeutic potential and research progress of diosgenin for lipid metabolism diseases. Drug Dev Res. 2022;83(8):1725–38. doi:10.1002/ddr.21991.
17. Hao Y, Gao X. Diosgenin protects retinal pigment epithelial cells from inflammatory damage and oxidative stress induced by high glucose by activating AMPK/Nrf2/HO-1 pathway. Immun Inflamm Dis. 2022;10(12):e698. doi:10.1002/iid3.698.
18. Diao Y. Clematichinenoside AR alleviates foam cell formation and the inflammatory response in Ox-LDL-induced RAW264.7 cells by activating autophagy. Inflammation. 2021;44(2):758–68. doi:10.1007/s10753-020-01375-x.
19. Liu Y, Uruno A, Saito R, Matsukawa N, Hishinuma E, Saigusa D, et al. Nrf2 deficiency deteriorates diabetic kidney disease in Akita model mice. Redox Biol. 2022;58(1):102525. doi:10.1016/j.redox.2022.102525.
20. Luo T, Jia X, Feng WD, Wang JY, Xie F, Kong LD, et al. Bergapten inhibits NLRP3 inflammasome activation and pyroptosis via promoting mitophagy. Acta Pharmacol Sin. 2023;44(9):1867–78. doi:10.1038/s41401-023-01094-7.
21. Sagoo MK, Gnudi L. Diabetic nephropathy: an overview. Methods Mol Biol. 2020;2067:3–7.
22. Zang N, Cui C, Guo X, Song J, Hu H, Yang M, et al. cGAS-STING activation contributes to podocyte injury in diabetic kidney disease. iScience. 2022;25(10):105145.
23. Fu Y, Sun Y, Wang M, Hou Y, Huang W, Zhou D, et al. Elevation of JAML promotes diabetic kidney disease by modulating podocyte lipid metabolism. Cell Metab. 2020;32(6):1052–62.e8.
24. Yang X, Tohda C. Diosgenin restores memory function via SPARC-driven axonal growth from the hippocampus to the PFC in Alzheimer's disease model mice. Mol Psychiatry. 2023;28(6):2398–411.
25. Chen MY, Tsai BC, Kuo WW, Kuo CH, Lin YM, Hsieh DJ, et al. Diosgenin attenuates myocardial cell apoptosis triggered by oxidative stress through estrogen receptor to activate the PI3K/Akt and ERK axes. Am J Chin Med. 2023;51(5):1211–32.
26. Zhong Y, Wang L, Jin R, Liu J, Luo R, Zhang Y, et al. Diosgenin inhibits ROS generation by modulating NOX4 and

mitochondrial respiratory chain and suppresses apoptosis in diabetic nephropathy. Nutrients. 2023;15(9):2164.

27. Sargazi Z, Yazdani Y, Tahavvori A, Youshanlouei HR, Alivirdiloo V, Beilankouhi EAV, et al. NFR2/ABC transporter axis in drug resistance of breast cancer cells. Mol Biol Rep. 2023;50(6):5407–14.
28. Bekyarova GY, Vankova DG, Madjova VH, Bekyarov NA, Salim AS, Ivanova DG, et al. Association between Nfr2, HO-1, NF-kB expression, plasma ADMA, and oxidative stress in metabolic syndrome. Int J Mol Sci. 2023;24(23):17067.
29. Li S, Zheng L, Zhang J, Liu X, Wu Z. Inhibition of ferroptosis by up-regulating Nrf2 delayed the progression of diabetic nephropathy. Free Radic Biol Med. 2021;162:435–49.
30. Aghelan Z, Pashaee S, Abtahi SH, Karima S, Khazaie H, Ezati M, et al. Natural immunosuppressants as a treatment for chronic insomnia targeting the inflammatory response induced by NLRP3/caspase-1/IL-1β axis activation: a scooping review. J Neuroimmune Pharmacol. 2023;18(3):294–309.
31. Liu Q, Zhang MM, Guo MX, Zhang QP, Li NZ, Cheng J, et al. Inhibition of microglial NLRP3 with MCC950 attenuates microglial morphology and NLRP3/Caspase-1/IL-1β signaling in stress-induced mice. J Neuroimmune Pharmacol. 2022;17(3–4):503–14. doi:10.1007/s11481-021-10037-0.
32. Zu Y, Mu Y, Li Q, Zhang ST, Yan HJ. Icariin alleviates osteoarthritis by inhibiting NLRP3-mediated pyroptosis. J Orthop Surg Res. 2019;14(1):307. doi:10.1186/s13018-019-1307-6.
33. Xiao Y, Zhao C, Tai Y, Li B, Lan T, Lai E, et al. STING mediates hepatocyte pyroptosis in liver fibrosis by Epigenetically activating the NLRP3 inflammasome. Redox Biol. 2023;62:102691. doi:10.1016/j.redox.2023.102691.
34. Wang W, Xiong Y, Zhao H, Xu R. CircEXOC5 facilitates cell pyroptosis via epigenetic suppression of Nrf2 in septic acute lung injury. Mol Cell Biochem. 2023;478(4):743–54. doi:10.1007/s11010-022-04521-1.
35. Kang JY, Xu MM, Sun Y, Ding ZX, Wei YY, Zhang DW, et al. Melatonin attenuates LPS-induced pyroptosis in acute lung injury by inhibiting NLRP3-GSDMD pathway via activating Nrf2/HO-1 signaling axis. Int Immunopharmacol. 2022;109(2):108782. doi:10.1016/j.intimp.2022.108782.
36. Lin Y, Luo T, Weng A, Huang X, Yao Y, Fu Z, et al. Gallic acid alleviates gouty arthritis by inhibiting NLRP3 inflammasome activation and pyroptosis through enhancing Nrf2 signaling. Front Immunol. 2020;11:580593.
37. Cloer EW, Goldfarb D, Schrank TP, Weissman BE, Major MB. NRF2 activation in cancer: from DNA to protein. Cancer Res. 2019;79(5):889–98.

Appendix A

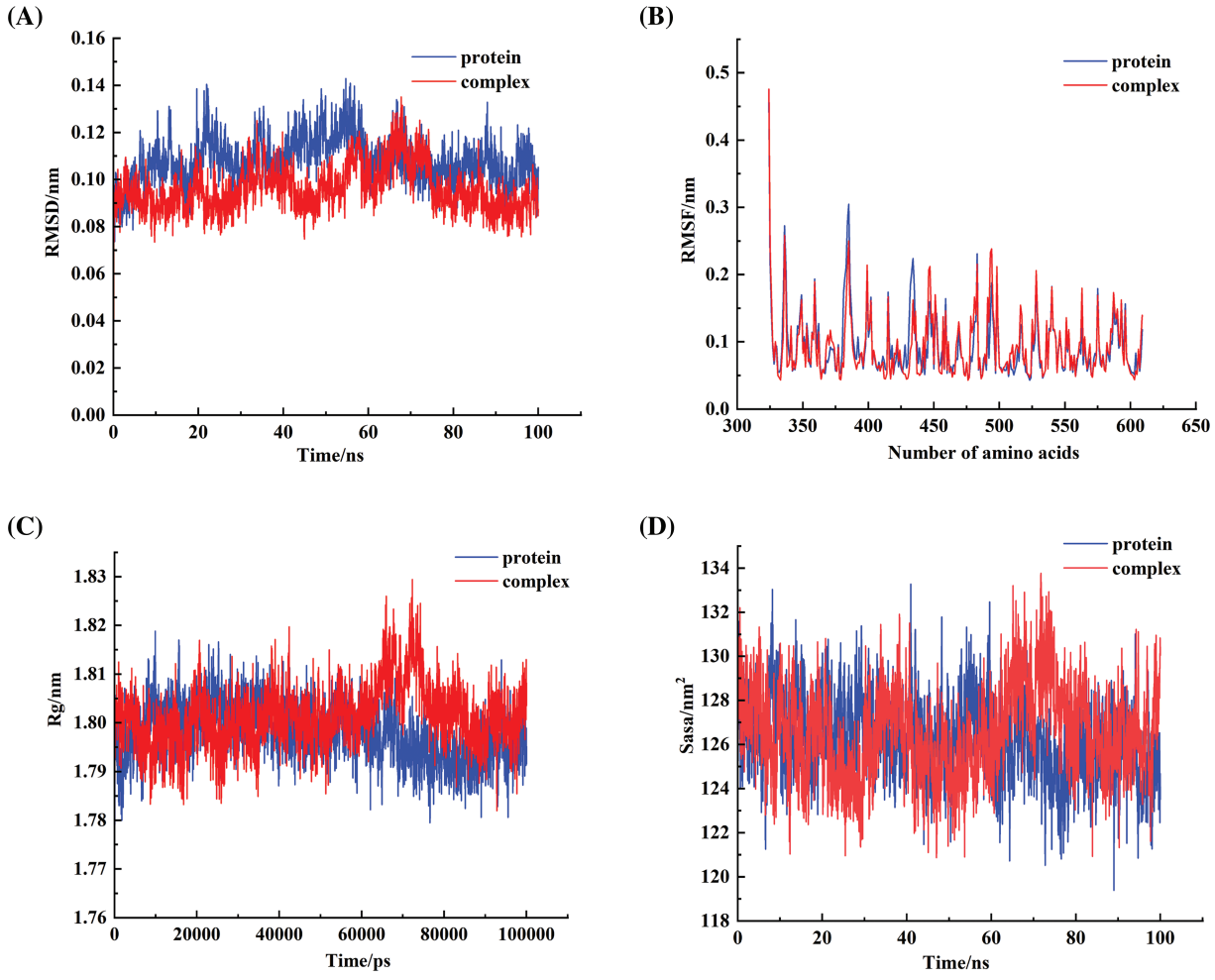

FIGURE A1. Simulation of the binding of diosgenin with Nrf2 using molecular dynamics methods. (A) The results of the RMSD value of the Nrf2-Diosgenin complex. (B) The results of the RMSF value of the Nrf2-Diosgenin complex. (C) The results of the Rg value of the Nrf2-Diosgenin complex. (D) The results of the SASA value of the Nrf2-Diosgenin complex.